Available online at www.sciencedirect.com

ScienceDirect

Inorganica Chimica Acta 361 (2008) 2462–2470

Inorganica Chimica Acta

www.elsevier.com/locate/ica

Chalcogenolato-bridged cyclometallated binuclear palladium complexes: Synthesis, spectroscopy, structures of $[Pd_2(\mu\text{-}Cl)(\mu\text{-}SMes)(C_{10}H_6NMe_2\text{–}C,N)_2]$ and $[Pd_2(\mu\text{-}SePh)_2(C_{10}H_6NMe_2\text{–}C,N)_2]$

Ninad D. Ghavale [a], Sandip Dey [a,*], Vimal K. Jain [a,*], M. Nethaji [b]

[a] *Chemistry Division, Bhabha Atomic Research Centre, Mumbai 400 085, India*
[b] *Department of Inorganic and Physical Chemistry, Indian Institute of Science, Bangalore 560 012, India*

Received 27 September 2007; received in revised form 8 January 2008; accepted 11 January 2008
Available online 19 January 2008

Abstract

Reactions of orthometallated binuclear palladium complexes with NaER, obtained by $NaBH_4$ reduction of R_2E_2 in methanol, gave complexes, $[Pd_2(\mu\text{-}ER)_2(C^\frown Y)_2]$ ($HC^\frown Y$ = *N*,*N*-dimethylbenzylamine ($C_6H_5CH_2NMe_2$), *N*,*N*-dimethylnaphthylamine ($C_{10}H_7NMe_2$), tri-*o*-tolylphosphine {P(tol-*o*)$_3$}; ER=SePh, SeMes, TePh, TeMes (Mes = 2,4,6-$Me_3C_6H_2$). Similar reactions of $[Pd_2(\mu\text{-}Cl)_2(C_{10}H_6NMe_2\text{–}C,N)_2]$ with $Pb(SMes)_2$ or MesSH in the presence of $NaHCO_3$ gave chloro/thiolato-bridged complex $[Pd_2(\mu\text{-}Cl)(\mu\text{-}SMes)(C_{10}H_6NMe_2\text{–}C,N)_2]$. The newly synthesized complexes were characterized by elemental analysis, UV–Vis, IR, NMR (^1H, ^{13}C, ^{31}P, ^{77}Se, ^{125}Te) spectroscopy. These complexes crystallized out preferentially in sym-*cis* configuration. A low energy charge transfer transition has been identified from chalcogenolate centers to an empty π^* orbital of cyclometallated ligand in absorption spectroscopy in these complexes. The structures of $[Pd_2(\mu\text{-}Cl)(\mu\text{-}SMes)(C_{10}H_6NMe_2\text{–}C,N)_2]$ (**1**) and $[Pd_2(\mu\text{-}SePh)_2(C_{10}H_6NMe_2\text{–}C,N)_2]$ (**3**) have been established by single crystal X-ray diffraction analyses. In the former, the two palladium atoms are held together by chloro and thiolato bridges whereas in the latter, the two phenylselenolato ligands bridge two palladium atoms. The pyrolysis of $[Pd(\mu\text{-}TeMes)(C_{10}H_6NMe_2\text{–}C,N)]_2$ (**10**) in a furnace gave Pd_7Te_3 whereas thermolysis in TOPO afforded primarily $PdTe_2$.

© 2008 Elsevier B.V. All rights reserved.

Keywords: Palladium; Orthometallation; Organochalcogenolates; Structures; NMR

1. Introduction

Cyclometallated palladium complexes have been investigated extensively [1] since the early study by Cope and Siekman [2]. There are several obvious reasons for this sustained interest in these complexes. These include their outstanding applications in organic synthesis [3], metallomesogenic as well as intriguing photophysical properties [4,5] and rich reaction chemistry [1]. Three general reactions, viz.: (i) bridge cleavage by neutral donor ligands, (ii) reactions involving metal–carbon bond, and (iii) substitution of the bridging ligands, have been reported for chloro/acetato-bridged palladium complexes. The latter reaction has been exploited to generate numerous mono- and bi-nuclear derivatives. The nature of incoming anionic ligand governs the overall nuclearity and stereochemistry of the complexes. Thus bidentate anionic ligands (L–L) such as acac$^-$, $(RO)_2PS_2^-$, and $R_2NCS_2^-$ yield mononuclear complexes with chelating L–L [1,6], whereas small bite anionic ligands, like 2-pyS$^-$, afford binuclear complexes e.g., $[Pd_2(\mu\text{-}Spy)_2(C^\frown N)_2]$ ($C^\frown N = C_6H_4CH_2NMe_2$) [7]. However, with simple thiolate ligands, only mono-substituted derivatives $[Pd_2(\mu\text{-}SR)(\mu\text{-}X)(C^\frown N)_2]$ (R = *n*-alkyl, Bu^t, Ph, *p*-tol; X = Cl, OAc, O_2CCF_3; $C^\frown N = RC_6H_3CH{=}NC_6H_4R'$,

---

[*] Corresponding authors. Tel.: +91 22 25592589.
E-mail addresses: dsandip@barc.gov.in (S. Dey), jainvk@barc.gov.in (V.K. Jain).

0020-1693/$ - see front matter © 2008 Elsevier B.V. All rights reserved.
doi:10.1016/j.ica.2008.01.005

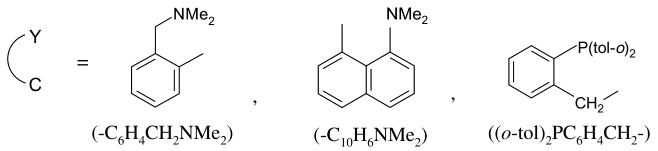

Scheme 1.

$CH_2C_9H_6N$) [8–10], rather than the disubstituted complexes, [$Pd_2(\mu\text{-}SR)_2(C^{\cap}N)_2$], could be isolated. This is in contrast to the fact that both classical and organometallic complexes, [$Pd_2X_2(\mu\text{-}ER')_2(PR_3)_2$] (X = Cl, Me; E = S or Se), can be prepared conveniently in high yields [11–13]. Thus, we have examined the reactions of orthopalladated compounds derived from nitrogen and phosphorus ligands (Scheme 1) with organochalcogenolate ions (RE^-; E = S, Se, Te) in the hope of isolating bis(organochalcogenolate)-bridged complexes. The heavier chalcogens (E = Se or Te) did afford "$Pd_2(\mu\text{-}ER)_2$" bridged complexes. The results of this work are reported herein.

2. Results and discussion

2.1. Synthesis and NMR spectroscopy

The reaction of [$Pd_2(\mu\text{-}Cl)_2(C_{10}H_6NMe_2\text{–}C,N)_2$] either with $Pb(SMes)_2$ or MesSH (Mes = 2,4,6-$Me_3C_6H_2$) in the presence of sodium bicarbonate gave a single molecular species, which was characterized as sym-*cis*-[$Pd_2(\mu\text{-}Cl)(\mu\text{-}SMes)(C_{10}H_6NMe_2\text{–}C,N)_2$] (**1**) by microanalysis, NMR and X-ray structural analysis. Treatment of [$Pd_2(\mu\text{-}X)_2(C^{\cap}Y)_2$] with NaER in benzene–methanol mixture afforded yellow to orange-red bis(organochalcogenolato)-bridged complexes, [$Pd_2(\mu\text{-}ER)_2(C^{\cap}Y)_2$] (ER = SePh, SeMes, TePh or TeMes) (Scheme 2). It is surprising that the thiolato ligands afford mono-thiolato bridged complexes, as reported earlier [8–10] and also observed during this investigation, while the heavier chalcogenolate conveniently yields bis-RE (E = Se or Te) bridged derivatives. This difference in reactivity may be attributed either to higher nucleophilicity and higher donation ability of SeR/TeR ligands than the RS^- group or relative size of the chalcogen atoms. The effect of the latter is reflected in Pd···Pd separation, which is 3.46 Å for **1** and 3.61 Å for **3**. The longer Pd···Pd separation in **3** possibly helps in reducing interatomic repulsion among organo groups attached to chalcogen atom and metallated ligand. The stability of M–E bond in several transition metal complexes increased in the order Te ≫ Se > S [14].

The complexes containing metallated nitrogen ligand were formed exclusively in sym-*cis* configuration. Accordingly in ^1H NMR spectra (Table 1), two separate resonances for EMes protons are observed. The 2,6-methyl signals appeared either as two closely spaced singlets or slightly broadened singlet. Similarly $^{77}Se\{^1H\}$ NMR spectrum of **3** exhibited two separate signals at δ −10.7 and −193.3 ppm; the former is assigned to SePh group *trans* to nitrogen while the latter *trans* to the metallated carbon atom of dimethylbenzylamine.

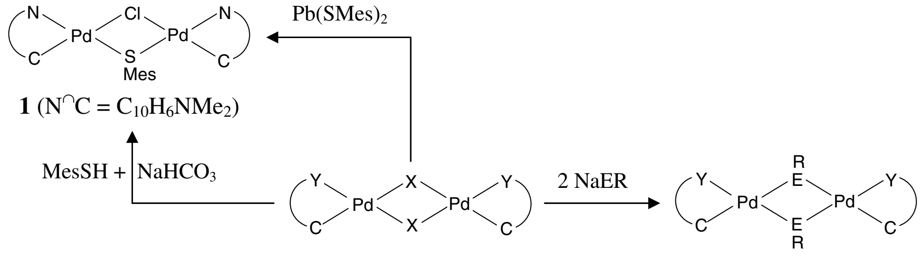

Y∩C	ER	
$C_6H_4CH_2NMe_2$	SePh	**2**
$C_{10}H_6NMe_2$	SePh	**3**
$(o\text{-tol})_2PC_6H_4CH_2$	SePh	**4**
$C_6H_4CH_2NMe_2$	SeMes	**5**
$C_{10}H_6NMe_2$	SeMes	**6**
$(o\text{-tol})_2PC_6H_4CH_2$	SeMes	**7**
$C_{10}H_6NMe_2$	TePh	**8**
$(o\text{-tol})_2PC_6H_4CH_2$	TePh	**9**
$C_{10}H_6NMe_2$	TeMes	**10**
$(o\text{-tol})_2PC_6H_4CH_2$	TeMes	**11**

Scheme 2.

Table 1
Electronic and NMR spectral data for organochalcogenolato-bridged orthometalled palladium(II) complexes

Complex	NMR δ in ppm		UV–Vis[a]
	^{1}H	^{13}C{^{1}H}	
[Pd_2(μ-Cl)$_2$($C_6H_4CH_2NMe_2$–C,N)$_2$]	2.79, 2.86 (NMe_2); 3.93 (NCH_2); 6.85–7.18 (m, C_6H_4)	52.7 (NMe_2); 73.4 (CH_2–); 121.4; 124.7; 125.1; 133.2; 142.9 (C-2); 146.9 (C–Pd)	340
[Pd_2(μ-Cl)$_2$($C_{10}H_6NMe_2$–C,N)$_2$]	3.45, 3.49 (NMe_2); 7.17–7.25 (m); 7.31–7.41 (m); 7.51 (d, 8 Hz); 7.61 (d, 8 Hz)	54.4, 54.8 (each s, NMe_2); 115.2; 123.2; 125.3; 126.2; 127.4; 129.0; 129.5; 134.8; 140.7; 155.4	301; 316; 327
[Pd_2(μ-OAc)$_2$(P-tol$_2C_6H_4CH_2$–C,P)$_2$][b]	1.95 (s, MeCOO); 2.60 (br, tol); 6.81–7.23 (m, tol)	22.2 (tol-Me); 24.1 (OAc); 30.2 (CH_2Pd); 125.1; 127.3 (d, 25 Hz quart C); 130 (d, 53 Hz quart C); 142.0; 157.2 (d, 32 Hz, quart C), 180.1 (br, C=O)	357
sym-*cis*-[Pd_2(μ-Cl)(μ-SMes)($C_{10}H_6NMe_2$–C,N)$_2$] (**1**)	2.21 (s, SMes, Me-4); 3.30 (s, SMes, Me-2,6); 3.38 (s, NMe_2); 6.67 (d, 7.3 Hz, 2H); 6.93 (s, SMes+napthyl, 4H); 7.30–7.38 (m, 6H); 7.55 (d, 2.5 Hz, 2H)	21.0 (s, Me-4, MesS); 26.3 (s, Me-2,6, MesS); 52.6 (s, NMe_2); 115.5; 122.7; 124.9; 126.2; 127.3; 128.4 (C-3,5 MesS); 129.5; 130.3; 132.9 (C-1 MesS); 134.7; 136.8; 141.2 (C-4, MesS); 142.8; 143.8 (C-2,6/MesS); 154.9	
sym-*cis*-[Pd_2(μ-SePh)$_2$($C_6H_4CH_2NMe_2$–C,N)$_2$] (**2**)	2.50, 2.76 (s, NMe_2); 3.91 (s, CH_2–); 6.88–8.23 (m, Ph+C_6H_4)	50.8 (s, NMe_2); 72.2 (NCH_2–); 122.0; 124.1; 125.8; 126.4; 127.8; 128.2; 135.5; 135.9; 137.8; 145.4; 148.0 (Pd–C); 153.2	
sym-*cis*-[Pd_2(μ-SePh)$_2$($C_{10}H_6NMe_2$–C,N)$_2$] (**3**)[c]	3.28 (br, NMe_2); 6.96–7.16 (m, 6H); 7.32–7.49 (m, 6H); 7.62–7.76 (m, 4H); 8.01–8.18 (m, 2H); 8.21–8.35 (m, 4H)	52.9 (s, NMe_2); 115.3; 123.0; 124.8; 125.2; 126.1; 127.2; 130.9; 132.9; 141.5; 156.4. 125.9; 126.8; 128.2; 131.6; 132.0; 132.3; 136.3; 150.8 (due to SePh)	306 (30050); 318 (29920); 328 (29410)
sym-*cis*-[Pd_2(μ-SePh)$_2${P(*o*-tol)$_2C_6H_4CH_2$–C,P}$_2$] (**4**)[d]	2.47 (*cis*), 2.60 (*trans*) (each s, 2:1, tol-Me); 3.18 (*cis*), 3.41 (*trans*) (each s, tol-CH_2, 2:1); 6.81–7.44 (m, Ph+C_6H_4); 7.79 (d, 6.5 Hz)	23.5 (s, tol-Me); 33.2 (*trans*), 34.5 (*cis*) (each s, 1:2 ratio, tol-CH_2–); 124.8, 125.6, 127.2, 127.6, 127.8, 128.1, 129.5, 124.8–136.8 (peaks due to SePh+*p*-tol group) 142.1 (d, 11 Hz); 159.1 (d, 36 Hz, *trans*, PCH_2–); 159.3 (d, 35 Hz, *cis*, PCH_2–)	283 (39890); 300 (35000); 360 (19980)
[Pd_2(μ-SeMes)$_2$($C_6H_4CH_2NMe_2$–C,N)$_2$] (**5**)	2.24 (SeMes, 4-Me); 2.40 (NMe_2); 3.17 (SeMes, 2,6-Me); 3.74 (CH_2N); 6.64 (br); 6.81–6.87 (m); 7.36–7.39 (m)	20.8 (SeMes, 4-Me); 27.4, 28.1, 28.3 (SeMes, 2,6-Me); 50.9, 51.4 (each s, NMe_2); 72.3 (s, CH_2N); 121.4; 121.6; 123.8; 125.1; 128.4; 128.6; 128.7; 129.3; 129.9; 131.0; 133.2; 134.2; 134.8; 135.5; 142.3; 142.6; 143.0; 147.8; 148.0; 152.7	272 (41700); 322 (sh, 20805); 395 (10940)
[Pd_2(μ-SeMes)$_2$($C_{10}H_6NMe_2$–C,N)$_2$] (**6**)	2.18, 2.22 (SeMes, 4-Me); 3.04, 3.07 (SeMes, 2,6-Me); 3.15; 3.23; 3.39; 6.89 (s, CH, 3,5 Mes); 6.98–7.52 (m)	20.6 (SeMes, 4-Me); 27.6; 28.0; 28.4 (SeMes, 2,6-Me); 52.5, 53.1 (each s, NMe_2); 114.7; 122.3; 124.3; 126.2; 126.9; 128.1; 128.5; 134.5; 135.2; 135.6; 141.2; 142.5; 150.5; 156.0	258 (sh, 37245); 307 (36870); 318 (37310); 328 (36750)
[Pd_2(μ-SeMes)$_2${P(tol-*o*)$_2C_6H_4CH_2$–C,P}$_2$] (**7**)[e]	2.02; 2.22; 2.29; 2.34; 2.35; 2.39; 2.54; 2.91; 6.50–7.31 (m)	20.7 (SeMes, 4-Me); 23.1 (tol-Me); 26.3, 27.4 (SeMes, 2,6-Me *cis*); 33.1 (PCH_2); 35.0; 124.5–136.4; 142.6; 143.6; 159.4 (d, 34 Hz, *p*-CH_2).	280 (sh, 50625); 319 (62825); 338 (sh, 49125); 372 (32875)
[Pd_2(μ-TePh)$_2$($C_{10}H_6NMe_2$–C,N)$_2$] (**8**)	3.35, 3.40 (NMe_2); 6.83–6.94 (m, 4H); 7.06–7.15 (m, 3H); 7.31–7.39 (m, 6H); 7.59–7.69 (m, 4H); 7.94–8.00 (m, 2H); 8.18 (d, 7.6 Hz, 1H); 8.36–8.40 (m, 2H)	52.1 (s, NMe_2); 115.8; 123.0; 123.3; 124.8; 126.4; 127.1; 127.5; 128.4; 129.4; 135.4; 135.7; 137.7; 140.2; 142.3; 144.1; 155.1; 156.2	271 (sh, 28290); 307 (28330); 317 (27820); 327 (26155); 390 (14400)
[Pd_2(μ-TePh)$_2${P(tol-*o*)$_2C_6H_4CH_2$–C,P}$_2$] (**9**)[f]	2.39 (*cis*), 2.47 *trans* (2:1, tol-Me); 3.27 (*cis*), 3.49 (*trans*) (2:1, PCH_2); 6.70–7.50 (m); 7.75 (d, 7 Hz)	24.1 (s, tol-Me); 30.4 (*trans*), 31.7 (*cis*) (PCH_2); 109.9 (Te–C); 124.6–142.0 (peaks due to TePh+*p*-tol carbons); 159.9 (d), 160.2 (d)	328 (23595); 387 (17410); 441 (13558)
[Pd_2(μ-MesTe)$_2$($C_{10}H_6NMe_2$–C,N)$_2$] (**10**)	2.19, 2.22 (s, 4-Me, Mes); 2.18–3.35 (NMe_2+2,6-Me; Mes); 6.75–6.97, 7.37–7.83 (m, $C_{10}H_6$)		290 (42950); 305 (44310); 317 (42470); 327 (41558); 427 (16037)
[Pd_2(μ-MesTe)$_2$(P(*o*-tol)$_2C_6H_4CH_2$–C,P)$_2$] (**11**)[g]	1.97 (s, 4-Me, Mes); 2.18, 2.22, 2.27, 2.31 (each s, 2,6-Me, Mes); 2.35 (s, tol-Me); 2.78 (s, tol-CH_2); 6.52, 6.62 (each s, CH, Mes); 6.87–7.07, 7.36 (m, tol-)		257 (79944); 322 (52519); 377 (31556)

[a] Wavelengths λ_{max} at the absorption maxima in nm, molar extinction coefficients ε in M^{-1} cm^{-1}.
[b] ^{31}P{^{1}H} NMR ($CDCl_3$): 36.5 (s, br). IR: 1576 cm^{-1} (ν_{CO}).
[c] ^{77}Se{^{1}H} NMR ($CDCl_3$) δ −10.7, −193.3 ppm.
[d] ^{31}P{^{1}H} NMR ($CDCl_3$): 34.9 (*cis*), 35.7 (*trans*); ^{77}Se{^{1}H} NMR ($CDCl_3$) δ: 77.1 (t, 130 Hz), −220 (s, ppm).
[e] ^{31}P{^{1}H} NMR ($CDCl_3$): 32.8 (*cis*); 34.6 (*trans* isomer).
[f] ^{31}P{^{1}H} NMR ($CDCl_3$): 32.9 (*cis*); 34.1 (*trans*).
[g] ^{31}P{^{1}H} NMR ($CDCl_3$): 26.9 (*cis*); 39.5 (*trans*).

Unlike bis(chalcogenolate) complexes derived from metallated nitrogen ligands, the metallated *o*-tolylphosphine derivatives were formed as a mixture of *cis* and *trans* isomers with the predominance of the former. Accordingly, these complexes displayed two resonances in their ^{31}P NMR spectra. From the spectral integration it can be inferred that the *trans* isomer exists in 5–15% concentration. The ^{77}Se{^{1}H} NMR spectrum of **4** (Fig. 1) exhibited two sets of resonances attributable to *cis* configuration. The high frequency resonance appeared as a triplet due to coupling with two equivalent *trans* phosphine ligands ($^2J(^{77}\mathrm{Se}–^{31}\mathrm{P}) = 130$ Hz). The low frequency resonance, however, appeared as a singlet. The magnitude of *cis* $^2J(^{77}\mathrm{Se}–^{31}\mathrm{P})$ couplings is usually smaller than 10 Hz. The observed coupling constants are in conformity with the values reported for mono- and bi- nuclear palladium/platinum selenolate complexes [15,16]. The ^{77}Se NMR resonance, expected to appear as a doublet due to ^2J(Se–P) couplings, for the *trans* isomer could not be identified with confidence owing to the low concentration (~5% by ^{31}P NMR integration) of this isomer in solution. The formation of *trans* isomer with metallated phosphine may be due to comparable trans influence of P and E ligating atoms, as a consequence, thermodynamic stability of *cis* and *trans* isomers may not be significantly different.

2.2. UV–Vis absorption spectroscopy

All cyclometallated complexes have strong absorption bands ($\varepsilon = 10^4$ M^{-1} cm^{-1}) in the visible region in dichloromethane (Table 1). The observed transition at $\lambda_{\max} \leqslant 360$ nm may be assigned to the ligand-centered (LC) charge transfer transition of the cyclometallated ligand and dσ^*(Pd) → π^*(C$^\cap$Y) metal-to-ligand-charge-transfer (MLCT) transition [17,18]. All the bis(chalcogenolato)-bridged complexes exhibited one band between 360 and 427 nm (Fig. 2). This long wavelength band at $\lambda_{\max} \geqslant 360$ nm is tentatively assigned as charge transfer transition from the selenolato/tellurolato centers of chalcogenolate ligand to an empty π^* orbital of the cyclometallated ligand (LLCT).

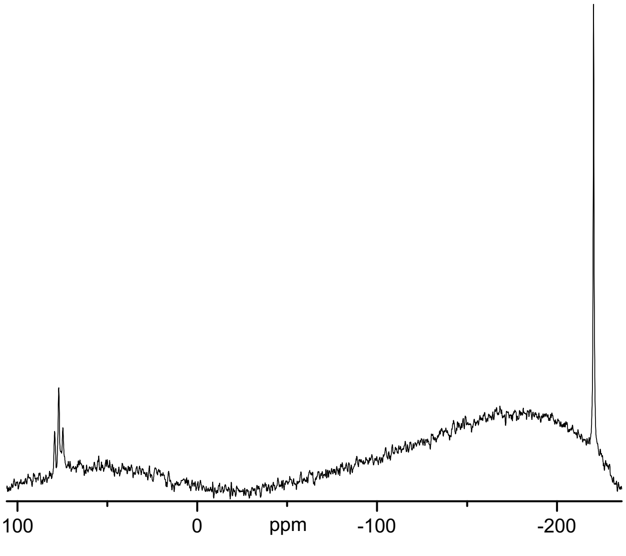

Fig. 1. ^{77}Se{^{1}H} NMR spectrum of [Pd$_2$(μ-SePh)$_2$(P(*o*-tol)$_2$C$_6$H$_4$CH$_2$–C,P)$_2$] (**4**).

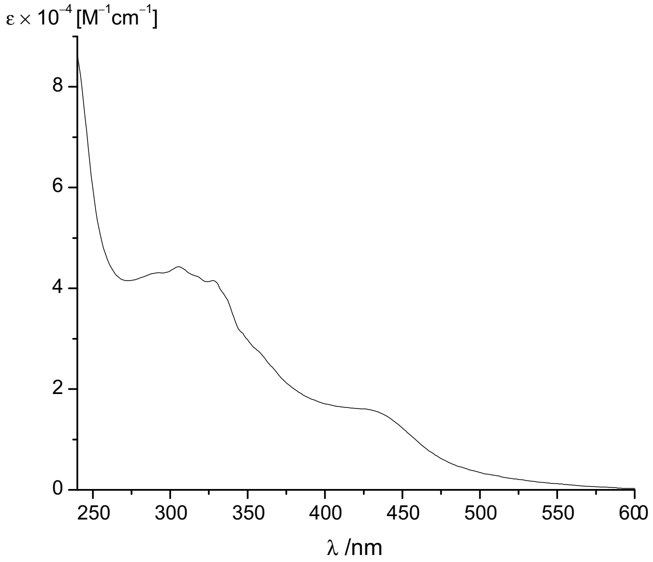

Fig. 2. UV–Vis spectrum of [Pd$_2$(μ-TeMes)$_2$(C$_{10}$H$_6$NMe$_2$–C,N)$_2$] (**10**) in CH$_2$Cl$_2$ solution.

For these binuclear palladium complexes of d^8 system, a dσ^* → π^* metal-metal-to-ligand-charge-transfer (MMLCT) is not preferred due to the absence of ground state metal–metal interaction. The Pd···Pd distance of 3.61 Å for **3** is too long to favor any inter-metal communication [17]. Also no ligand-field d–d transition is expected in the observed spectral region. The two strong ligands, viz., cyclometallated and heavier chalcogen, can cause only very weak but high energy ligand-field d–d transitions appearing below 360 nm [18].

The tellurolato-bridged complexes have their absorption band at lower energies at about 427 nm (**10**) as compared to about 395 nm (**5**) for the Se complexes. In chemical terms, the replacement of Se by stronger σ donor Te destabilizes the HOMO causing the bathochromic shift [19,20]. A hypsochromic shift of about 50 nm wavelength absorption is also observed in case of phosphine complexes. This may be rationalized by the stronger back bonding interaction between Pd$^{\mathrm{II}}$ and the phosphine acceptor destabilizing the LUMO (π^*), which is responsible for the blue shift. In the analogous Pd/Te/naphthylamine complexes, the increasing donor strength of mesityl group due to three methyl groups in benzene ring is reflected in red shift of $\lambda_{\max}$ when compared between complexes **8** (390 nm) and **10** (427 nm). This long wavelength band for Pd/Se/naphthylamine complexes could not be marked. This may be presumably due to blue shifting of the absorption as compared to corresponding Te analogues, which are masked in the tailing of highly intense typical three bands at ~306, 318 and 328 nm of naphthylamine complexes of Pd(II).

2.3. Crystallography

The molecular structures of $[Pd_2(\mu\text{-Cl})(\mu\text{-SMes})(C_{10}H_6\text{-}NMe_2\text{–}C,N)_2]$ (**1**) and $[Pd_2(\mu\text{-SePh})_2(C_{10}H_6NMe_2\text{–}C,N)_2]$ (**3**) were established by single crystal X-ray diffraction analyses. The ORTEP [21] drawings with atomic numbering scheme are shown in Figs. 3 and 4, and the selected bond lengths and angles are given in Tables 2 and 3, respectively.

Table 2
Selected bond lengths (Å) and angles (°) for $[Pd_2(\mu\text{-Cl})(\mu\text{-SMes})(C_{10}H_6NMe_2\text{–}C,N)_2]$ (**1**)

Pd(1)–C(9)	1.982(7)	Pd(2)–C(21)	1.982(8)
Pd(1)–N(1)	2.128(6)	Pd(2)–N(2)	2.136(7)
Pd(1)–S(1)	2.303(2)	Pd(2)–S(1)	2.307(2)
Pd(1)–Cl(1)	2.485(2)	Pd(2)–Cl(1)	2.469(2)
C(1)–N(1)	1.474(10)	C(13)–N(2)	1.483(10)
S(1)–C(25)	1.802(7)	C(26)–C(31)	1.497(10)
C(9)–Pd(1)–N(1)	83.4(3)	C(21)–Pd(2)–N(2)	84.1(3)
C(9)–Pd(1)–S(1)	96.5(2)	C(21)–Pd(2)–S(1)	95.2(2)
C(9)–Pd(1)–Cl(1)	173.5(2)	C(21)–Pd(2)–Cl(1)	177.3(2)
N(1)–Pd(1)–Cl(1)	93.52(17)	N(2)–Pd(2)–Cl(1)	93.57(19)
N(1)–Pd(1)–S(1)	178.03(18)	N(2)–Pd(2)–S(1)	178.83(19)
S(1)–Pd(1)–Cl(1)	86.79(7)	S(1)–Pd(2)–Cl(1)	87.10(7)
Pd(1)–S(1)–C(25)	109.3(2)	Pd(2)–S(1)–C(25)	108.3(2)
Pd(1)–N(1)–C(1)	108.9(5)	Pd(2)–N(2)–C(13)	108.2(5)
Pd(1)–S(1)–Pd(2)	97.29(7)	Pd(1)–Cl(1)–Pd(2)	88.63(7)

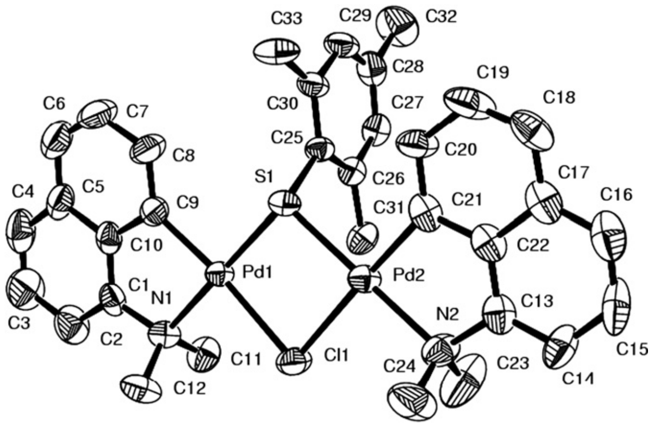

Fig. 3. Molecular structure of $[Pd_2(\mu\text{-Cl})(\mu\text{-SMes})(C_{10}H_6NMe_2\text{–}C,N)_2]$ (**1**). H atoms were omitted for clarity.

Complex **1** has a sym-*cis* configuration with the nitrogen atoms *trans* to the bridging thiolato ligand. A similar configuration has been reported for $[Pd_2(\mu\text{-Cl})(\mu\text{-SBu}^n)\text{-}\{(Bu^nO)C_6H_3CH{=}NC_6H_4(OBu^n\text{-}4)\}_2]$ [9], $[Pd_2(\mu-OAc)(\mu-SBu^n)\{(Bu^n_2N)C_6H_3CH{=}NC_6H_4NO_2-4\}_2]$ [10] and $[Pd_2(\mu\text{-}O_2CCF_3)(\mu\text{-SBu}^t)($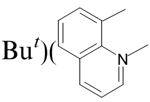$)_2]$ [8]. The two palladium–carbon distances are similar and are well in agreement to those found in cyclopalladated amine complexes [6,10]. The two Pd–S bond lengths are comparable and are within the range reported for bridging thiolato complexes [22,23]. The Pd–N distances are slightly shorter than the mixed carboxylato–thiolato bridged derivatives $[Pd_2(\mu\text{-}O_2CR)(\mu\text{-SR}')(C^\cap N)_2]$ [8,10], but are similar to the one observed for $[Pd_2(\mu\text{-Cl})(\mu\text{-SBu}^n)\{(Bu^nO)C_6H_3CH{=}NC_6H_4\text{-}(OBu^n\text{-}4)\}_2]$ [9].

The metallated *N*,*N*′-dimethylnapthylamine forms a planar five-membered $N^\cap C$ chelate ring with bite angle of ~84°, which can be compared with the angle reported for

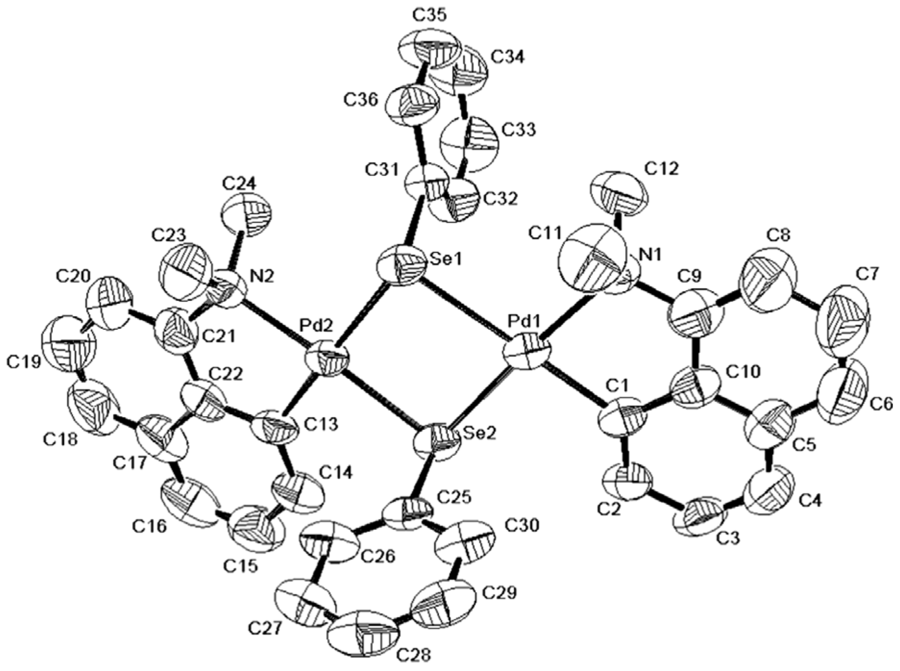

Fig. 4. Molecular structure of $[Pd_2(\mu\text{-SePh})_2(C_{10}H_6NMe_2\text{–}C,N)_2]$ (**3**). H atoms were omitted for clarity.

Table 3
Selected bond lengths (Å) and angles (°) for $[Pd_2(\mu\text{-}SePh)_2(C_{10}H_6NMe_2\text{-}C,N)_2]$ (**3**)

Pd(1)–C(1)	2.009(5)	Pd(2)–C(13)	1.991(5)
Pd(1)–N(1)	2.153(4)	Pd(2)–N(2)	2.151(4)
Pd(1)–Se(1)	2.5522(7)	Pd(2)–Se(1)	2.5543(7)
Pd(1)–Se(2)	2.3881(7)	Pd(2)–Se(2)	2.3874(7)
Se(1)–C(31)	1.937(5)	Se(2)–C(25)	1.936(5)
N(1)–C(9)	1.478(7)	N(2)–C(21)	1.466(7)
N(1)–Pd(1)–Se(1)	98.18(11)	N(2)–Pd(2)–Se(1)	98.21(12)
C(1)–Pd(1)–Se(2)	94.22(16)	C(13)–Pd(2)–Se(2)	94.02(16)
C(1)–Pd(1)–Se(1)	177.69(15)	Se(1)–Pd(2)–C(13)	178.60(16)
N(1)–Pd(1)–C(1)	83.10(19)	N(2)–Pd(2)–C(13)	83.2(2)
Se(1)–Pd(1)–Se(2)	84.62(2)	Se(1)–Pd(2)–Se(2)	84.59(2)
Se(2)–Pd(2)–N(2)	176.97(11)	Pd(1)–Se(2)–Pd(2)	98.18(2)
Pd(1)–Se(1)–Pd(2)	89.94(2)	Pd(1)–Se(2)–C(25)	102.51(16)
Pd(1)–Se(1)–C(31)	99.23(15)	Pd(2)–Se(2)–C(25)	102.35(15)
Pd(2)–Se(1)–C(31)	100.64(15)		

cyclometallated amine ligands [8–10]. The chelated metallated rings and four-membered Pd_2SCl ring are co-planar. The S–Pd–Cl angles are significantly smaller than the ideal value (90°) indicating strain in the four-membered ring. Consequently, S–Pd–C and Cl–Pd–N angles have opened up. The Pd–S–Pd angle is within the range reported for thiolato-bridged complexes (79–102°) [8–10,24].

Complex **3** consists of two distorted square planar palladium atoms, which are held together by two phenylselenolato bridges. The phenyl groups of the PhSe ligand adopt an *anti* configuration. The molecule has a sym-*cis* configuration with a non-planar four-membered Pd_2Se_2 ring, as observed in $[Pt_2Cl_2(\mu\text{-}SeBz)_2(PPr_3)_2]$ [25]. However, in other selenolato-bridged phosphine derivatives, $[M_2Cl_2(\mu\text{-}SeR')_2(PR_3)_2]$ (M/R′/R = Pd/CH_2CH_2COOMe/Ph [26], Pt/Et/Et [27]), the four-membered M_2Se_2 ring is planar. The five membered metallated amine is in plane with the coordination plane of the palladium.

There are two distinct Pd–Se bonds (Table 3). The bond *trans* to carbon is longer (~0.17 Å) than the one *trans* to nitrogen reflecting strong *trans* influence of the metallated carbon. These distances can be compared with those reported for $[M_2Cl_2(\mu\text{-}SeR')_2(PPr_3)_2]$ [25–27] and other related derivatives [28–31]. The Pd–N distances (2.15 Å) are slightly longer than those reported in $[Pd_2Cl_2(\mu\text{-}Me_2pz)_2(PMe_2Ph)_2]$ (Pd–N = 2.03–2.08 Å) [32], $[Pd_3(\mu\text{-}pz)_6]$ ($Pd\text{–}N_{av}$ = 2.00 Å) [33], but are closer to mononuclear complex $[PdCl(SeCH_2CH_2NMe_2)(PPh_3)]$ (Pd–N = 2.16 Å) [34]. The Pd–C distances are in good agreement with reported values [6,24]. Various angles around palladium atoms and in the four-membered Pd_2Se_2 ring of **3** are similar to those observed for **1**.

2.4. Thermal studies

Thermogravimetric analysis of **10** was carried out under a flowing argon atmosphere. The TG curve of **10** showed two well separated steps of decomposition at 265 and 465 °C, respectively, leading to the formation of Pd_7Te_3 as inferred from the calculated weight loss and XRD pattern [35]. To prepare large quantities of the telluride, a substantial amount (100–200 mg) of complex **10** was heated in a furnace at 465 °C for 2 h under a dynamic dry argon atmosphere. The weight loss, XRD pattern and EDAX (*Anal.* Calc. for Pd_7Te_3: Pd, 66.1; Te, 33.9. Found: Pd, 62.6; Te, 37.4%) of the residue matched well with Pd_7Te_3 [35] as obtained from TG. To identify the intermediate product formed at 265 °C in TG, we have pyrolysed **10** in a preheated furnace at 265 °C for 2 h. The XRD pattern of this residue indicates the formation of a mixture of palladium tellurides, mainly Pd_9Te_4 and Pd_2Te. Pyrolysis of **10** in refluxing (202 °C) tri-*n*-octylphosphine oxide for 6 h gave a black residue, which has been identified as $PdTe_2$ from XRD pattern (supplementary material) [36]. Evidently depending on pyrolysis temperature, different palladium tellurides are formed seemingly by tellurium elimination on increasing temperature. Palladium is known to form several tellurides differing in stoichiometry and structures [37].

3. Conclusions

Binuclear cyclometallated palladium complexes containing bis-selenolato/tellurolato bridge have been synthesized conveniently. The *cis* and *trans* isomerism has been observed for cyclometallated phosphine derivatives with the predominance of the former, on the other hand cyclometallated heterocyclic nitrogen ligands afford the *cis* isomer exclusively. A charge transfer transition has been observed from chalcogen center to an empty π^* orbital of the cyclometallated ligand. The tellurolato derivatives have been demonstrated to serve as molecular precursors for the preparation of palladium tellurides.

4. Experimental

4.1. General

Elemental analysis were carried out on a Carlo-Erba EA-1110 CHN-O instrument. Melting points were determined in capillary tubes and are uncorrected. ^1H, $^{13}C\{^1H\}$, $^{31}P\{^1H\}$, $^{77}Se\{^1H\}$ and $^{125}Te\{^1H\}$ NMR spectra were recorded on a Bruker DPX-300 NMR spectrometer operating at 300, 75.47, 121.5, 57.24 and 94.86 MHz, respectively. Chemical shifts are relative to internal chloroform peak (δ 7.26 ^1H and 77.0 for ^{13}C) and external 85% H_3PO_4 for ^{31}P, external Me_2Se for $^{77}Se\{^1H\}$ (secondary reference Ph_2Se_2 in $CDCl_3$, δ 463 ppm) and $[Te(dtc)_2]$ ($\delta = 0$ ppm; dtc=*N*,*N*-diethyldithiocarbamate) for $^{125}Te\{^1H\}$ NMR spectra. A 90° pulse was used in every case. A weighting function was applied in $^{77}Se\{^1H\}$ and $^{125}Te\{^1H\}$ NMR spectra. Electronic spectra were recorded on a Chemito Spectrascan UV 2600 spectrophotometer. IR data were recorded on a Bomem MB-102 FT-IR spectrophotometer. TG curves were obtained at a heating rate of 10 °C min^{-1} under flowing argon on a Nitzsch STA

PC-Luxx TG-DTA instrument. EDAX were carried out with a Tescan Vega 2300T/40 instrument. Powder XRD patterns were recorded on a Philips PW1820 using Cu Kα radiation.

4.2. Materials

Solvents were dried and distilled under a nitrogen atmosphere prior to use according to literature method [38]. All reactions were carried out in Schlenk flask under a nitrogen atmosphere. *N*,*N*-dimethylbenzylamine, *N*,*N*-dimethylnaphthylamine, tri-*o*-tolylphosphine, MesBr (Mes = 2,4,6-$Me_3C_6H_2$), Ph_2Se_2 and other reagents were obtained from commercial sources and were used without further purification. Palladium precursors, $[Pd(OAc)_2]_3$ [39], $Na_2[PdCl_4]$ [40], $[Pd(\mu\text{-}Cl)(Y^{\cap}C)]_2$ ($Y^{\cap}CH$ = *N*,*N*-dimethylbenzylamine, *N*,*N*-dimethylnaphthylamine [41], tri-*o*-tolylphosphine [42]), Mes_2S_2 [43], Mes_2Se_2 [44], Mes_2Te_2 [45] and Ph_2Te_2 [46] were prepared according to literature methods.

4.3. Preparations

4.3.1. Bis(mesitylthiolato)lead(II)

To a benzene solution of NaSMes [prepared by $NaBH_4$ (388 mg, 10.2 mmol), reduction of dimesityl disulphide (1.502 g, 4.9 mmol) in methanol], a solution of $Pb(OAc)_2$ (1.882 g, 4.9 mmol) in methanol was added and stirred for 4 h at room temperature whereupon a yellow-brown precipitate formed, which was filtered and washed with methanol, water, acetone and ether. The solid was dried in vacuo (516 mg, 20%, m.p. 250 °C).

4.3.2. μ-Chloro-μ-mesitylthiolatobis[(N,N-dimethylnapthylamine-2C,N)]dipalladium(II) (*1*)

(a) To a benzene solution of $[Pd_2(\mu\text{-}Cl)_2(C_{10}H_6NMe_2\text{–}C,N)_2]$ (242 mg, 0.38 mmol), $Pb(SMes)_2$ (205 mg, 0.40 mmol) was added with stirring at room temperature. The solution turned brown after few minutes. After stirring the solution for 4 h, the solvent was evaporated under vacuum and the residue was washed with hexane and ether and then was extracted with benzene. The extract was filtered and the filtrate was concentrated to 5 cm^3 followed by the addition of hexane (3 cm^3) to precipitate a yellow solid, which was filtered out and recrystallised from dichloromethane–acetone–hexane (171 mg, 60%).

(b) To a methanol solution of 2,4,6-trimethylthiophenol (52 mg, 0.34 mmol) containing $NaHCO_3$ (30 mg, 0.40 mmol), a solution of di-μ-chlorobis(*N*,*N*-dimethylnapthylamine-2C,N)dipalladium(II) (213 mg, 0.34 mmol) in benzene was added and stirred at room temperature for 4 h. The solvents were evaporated under vacuum and residue was washed with hexane and then was extracted with benzene. The extract was filtered and the filtrate was concentrated and a few cm^3 of hexane was added to yield a yellow solid (50 mg, 40%). UV–Vis (CH_2Cl_2) λ_{max} in nm: 290 (25250); 302 (22880); 316 (18875); 327 (15625); 350 (sh, 9550). ^1H NMR was consistent with the spectrum obtained for the sample prepared via route (a).

4.3.3. Di-μ-phenylselenolatobis[o-(di-o-tolylphosphino)benzyl]dipalladium(II) (*4*)

To a benzene solution (10 cm^3) of NaSePh (prepared by $NaBH_4$ (15 mg, 0.396 mmol), reduction of diphenyl diselenide (65 mg, 0.208 mmol) in methanol (3 cm^3)), a solution of *trans*-di(μ-acetato)-bis[*o*-(di-*o*-tolylphosphino)benzyl] dipalladium(II) (195 mg, 0.207 mmol) in benzene (10 cm^3) was added and stirred for 4 h at room temperature. The solvents were evaporated under vacuum and the residue was washed with hexane and extracted with benzene. The extract was passed through a Florisil column. The filtrate was concentrated and few drops of hexane were added to obtain a yellow solid (118 mg, 50%).

4.3.4. Di-μ-mesitylselenolatobis[(N,N-dimethylbenzylamine-2C,N)]dipalladium(II) (*5*)

To a benzene solution of NaSeMes (prepared by $NaBH_4$ (30 mg, 0.79 mmol), reduction of dimesityl diselenide (150 mg, 0.37 mmol) in methanol (3 cm^3)), a solution of di-μ-chlorobis(*N*,*N*-dimethylbenzylamine-2C,N) dipalladium(II) (208 mg, 0.37 mmol) in benzene (10 cm^3) was added and stirred for 4 h at room temperature. The solvents were evaporated under vacuum and residue was washed with hexane and extracted with benzene. The extract was passed through a Florisil column. The filtrate was concentrated in vacuo and few drops of hexane were added to obtain orange-red solid (98 mg, 30%). All other bi-nuclear complexes were prepared in a similar manner. Pertinent data are summarized in Table 4.

4.3.5. Di-μ-mesityltellurolatobis[(N,N-dimethylnapthylamine-2C,N)]dipalladium(II) (*10*)

A benzene (10 cm^3) solution of di-μ-chlorobis(*N*,*N*-dimethylnapthylamine-2C,N)dipalladium(II) (195 mg, 0.31 mmol) was added to a freshly prepared methanolic solution (10 cm^3) of NaTeMes (prepared by the reduction of dimesityl ditelluride (159 mg, 0.32 mmol) by methanolic $NaBH_4$ (26 mg, 0.68 mmol)), and stirred for 4 h at room temperature. The solvents were evaporated under vacuum, the residue was washed with hexane and extracted with benzene (3×10 cm^3). The extract was passed through a Florisil column. The volume of extract was reduced to 5 cm^3, few drops of hexane were added to yield (147 mg, 45%) a brown-red solid. M.p.: 160 °C (dec.). UV–Vis (CH_2Cl_2) λ_{max} in nm: 290 (42950); 305 (44310); 317 (42470); 327 (41558); 427 (16037).

4.4. Crystallography

The unit cell parameters and the intensity data for a yellow single crystals of **1** and **3** were collected at 0 and 20 °C,

Table 4
Physical and analytical data of chalcogenolato-bridged orthometallated palladium(II) complexes

Complex	Recrystallisation solvent (yield%)	M.p. (°C)	% Analysis Found (Calc.)		
			C	H	N
$[Pd_2(\mu\text{-Cl})(\mu\text{-SMes})(C_{10}H_6NMe_2\text{–C, N})_2]$ (**1**)[a]	dichloromethane–acetone–hexane (60)	237 (dec.)	54.2 (53.6)	5.0 (4.8)	4.1 (3.8)
$[Pd_2(\mu\text{-SePh})_2(C_6H_4CH_2NMe_2\text{–C,N})_2]$ (**2**)	benzene–hexane (40)	155	46.0 (45.4)	4.2 (4.3)	3.7 (3.5)
$[Pd_2(\mu\text{-SePh})_2(C_{10}H_6NMe_2\text{–C,N})_2]$ (**3**)	benzene–hexane (39)	153	49.4 (50.0)	3.8 (4.0)	3.4 (3.2)
$[Pd_2(\mu\text{-SePh})_2(P(o\text{-tol})_2C_6H_4CH_2\text{–C,P})_2]$ (**4**)	benzene–hexane (50)	121	57.3 (57.3)	4.3 (4.5)	
$[Pd_2(\mu\text{-SeMes})_2(C_6H_4CH_2NMe_2\text{–C,N})_2]$ (**5**)	benzene–hexane (43)	170	50.0 (49.3)	5.5 (5.3)	3.5 (3.2)
$[Pd_2(\mu\text{-SeMes})_2(C_{10}H_6NMe_2\text{–C,N})_2]$ (**6**)	benzene–hexane (55)	217	52.5 (53.1)	4.8 (4.9)	3.4 (3.2)
$[Pd_2(\mu\text{-SeMes})_2(P(o\text{-tol})_2C_6H_4CH_2\text{–C,P})_2]$ (**7**)	benzene–hexane (32)	222	58.7 (59.3)	5.0 (5.1)	
$[Pd_2(\mu\text{-TePh})_2(C_{10}H_6NMe_2\text{–C,N})_2]$ (**8**)	benzene–hexane (34)	129	45.3 (44.9)	3.4 (3.6)	2.8 (2.9)
$[Pd_2(\mu\text{-TePh})_2(P(o\text{-tol})_2C_6H_4CH_2\text{–C,P})_2]$ (**9**)	benzene–hexane (38)	135	51.8 (52.8)	3.7 (4.1)	
$[Pd_2(\mu\text{-TeMes})_2(C_{10}H_6NMe_2\text{–C,N})_2]$ (**10**)	benzene–hexane (45)	160 (dec)	48.0 (48.2)	4.3 (4.4)	3.0 (2.8)
$[Pd_2(\mu\text{-TeMes})_2(P(o\text{-tol})_2C_6H_4CH_2\text{–C,P})_2]$ (**11**)	benzene–hexane (34)	210	54.4 (54.9)	4.7 (4.8)	

[a] S: 4.1 (4.3).

Table 5
Crystallographic and structure refinement details for $[Pd_2(\mu\text{-Cl})(\mu\text{-SMes})(C_{10}H_6NMe_2\text{–C, N})_2]$ (**1**) and $[Pd_2(\mu\text{-SePh})_2(C_{10}H_6NMe_2\text{–C,N})_2]$ (**3**)

Chemical formula	$C_{33}H_{35}ClN_2Pd_2S$ (**1**)	$C_{36}H_{34}N_2Pd_2Se_2$ (**3**)
Formula weight	739.94	865.37
Crystal size (mm)	0.44 × 0.33 × 0.28	0.54 × 0.11 × 0.04
Crystal system	orthorhombic	monoclinic
Space group	*Pbca*	$P2_1/c$
Unit cell dimensions		
a (Å)	12.699(3)	12.6917(14)
b (Å)	21.659(6)	11.6796(12)
c (Å)	22.424(6)	22.584(2)
β (°)		95.040(2)
Volume (Å^3)	6168(3)	3334.8(6)
D_{calc} (g cm^{-1})	1.594	1.724
Z	8	4
μ (mm^{-1})/$F(000)$	1.345/2976	3.288/1696
θ Range for data collection (°)	1.82–27.99	1.81–27.70
Goodness of fit on F^2	0.733	0.988
Absorption correction	SADABS	SADABS
Reflections collected/unique	68573/7410	28384/7828
Data/restraints/parameters	7410/0/359	7828/0/383
Final R_1, wR_2 indices	0.051, 0.124	0.048, 0.087
R_1, wR_2 (all data)	0.121, 0.178	0.108, 0.106
Largest difference in peak and hole (e Å^{-3})	0.73	0.99

respectively, on a Bruker Smart Apex CCD diffractometer using graphite monochromated Mo Kα radiation ($\lambda = 0.71073$ Å), employing the ω–2θ scan technique. The intensity data were corrected for Lorentz, polarization and absorption effects. The structure was solved using the SHELXS97 [47] and refined using the SHELXL97 [48] computer programs. The non-hydrogen atoms were refined anisotropically. Selected crystallographic data are given in Table 5.

Acknowledgments

We thank Drs. T. Mukherjee and D. Das for the encouragement of this work. We are grateful to Dr. V.K. Manchanda, Head, Radiochemistry Division, BARC for providing microanalysis of the complexes.

Appendix A. Supplementary material

CCDC 651065 and 651066 contain the supplementary crystallographic data for $[Pd_2(\mu\text{-Cl})(\mu\text{-SMes})(C_{10}H_6NMe_2\text{–C,N})_2]$ (**1**) and $[Pd_2(\mu\text{-SePh})_2(C_{10}H_6NMe_2\text{–C,N})_2]$ (**3**). These data can be obtained free of charge from The Cambridge Crystallographic Data Centre via www.ccdc.cam.ac.uk/data_request/cif. Supplementary data associated with this article can be found, in the online version, at doi:10.1016/j.ica.2008.01.005.

References

[1] V.K. Jain, L. Jain, Coord. Chem. Rev. 249 (2005) 3075.
[2] A.C. Cope, R.W. Siekman, J. Am. Chem. Soc. 87 (1965) 3272.
[3] A.D. Ryabov, Synthesis (1985) 233.
[4] P. Espinet, M.A. Esteruelas, L.A. Oro, J.L. Serrano, E. Sola, Coord. Chem. Rev. 117 (1992) 215.
[5] A.P. Polishchuk, T.V. Timofeeva, Russian Chem. Rev. 62 (1993) 291.
[6] S. Narayan, V.K. Jain, R.J. Butcher, J. Organomet. Chem. 549 (1997) 73.
[7] A.J. Deeming, M.N. Meah, P.A. Bates, M.B. Hursthouse, J. Chem. Soc., Dalton Trans. (1988) 2193.
[8] J. Ruiz, N. Cutillas, J. Torregrosa, G. Garcia, G. Lopez, P.A. Chaloner, P.B. Hitchcock, R.M. Harrison, J. Chem. Soc., Dalton Trans. (1994) 2353.
[9] J. Buey, G.A. Diez, P. Espinet, S. Garcia-Granda, E. Perez-Carreno, Eur. J. Inorg. Chem. (1998) 1235.
[10] J. Buey, S. Coco, L. Diez, P. Espinet, J.M. Martin-Alvarez, J.A. Miguel, S. Garcia-Granda, A. Tesouro, I. Ledoux, J. Zyss, Organometallics 17 (1998) 1750.
[11] V.K. Jain, Inorg. Chim. Acta 133 (1987) 261.
[12] V.K. Jain, S. Kannan, J. Organomet. Chem. 439 (1992) 231.
[13] A. Singhal, V.K. Jain, J. Chem. Soc., Dalton Trans. (1993) 1515.
[14] W. Levason, G. Reid, in: J.A. McCleverty, T.J. Meyer (Eds.), Comprehensive Coordination Chemistry, vol. 1, Pergamon, Oxford, 2004, p. 395.
[15] S. Dey, V.K. Jain, A. Knoedler, W. Kaim, S. Zalis, Eur. J. Inorg. Chem. (2001) 2965.
[16] S. Dey, L.B. Kumbhare, V.K. Jain, T. Schurr, W. Kaim, A. Klein, F. Belaj, Eur. J. Inorg. Chem. (2004) 4510.

[17] S.-W. Lai, T.-C. Cheung, M.C.W. Chan, K.-K. Cheung, S.-M. Peng, C.-M. Che, Inorg. Chem. 39 (2000) 255.
[18] L. Chassot, A.V. Zelewsky, Inorg. Chem. 26 (1987) 2814.
[19] S. Dey, V.K. Jain, A. Knoedler, A. Klein, W. Kaim, S. Zalis, Inorg. Chem. 41 (2002) 2864.
[20] S. Dey, V.K. Jain, J. Singh, V. Trehan, K.K. Bhasin, B. Varghese, Eur. J. Inorg. Chem. (2003) 744.
[21] C.K. Johnson, ORTEP II-A FORTRAN Thermal Ellipsoid Plot Program for Crystal Structure Illustrations, ORNL-5138, 1976.
[22] I. Schneider, M. Hörner, R.N. Olendzki, J. Strähle, Acta Cryst. C49 (1993) 2091.
[23] V.K. Jain, R.P. Patel, K.V. Muralidharan, R. Bohra, Polyhedron 8 (1989) 2151.
[24] V.K. Jain, R.P. Patel, K. Venkatasubramanian, Polyhedron 10 (1991) 851.
[25] S. Dey, V.K. Jain, B. Varghese, J. Organomet. Chem. 623 (2001) 48.
[26] L.B. Kumbhare, V.K. Jain, P.P. Phadnis, M. Nethaji, J. Organomet. Chem. 692 (2007) 1546.
[27] V.K. Jain, S. Kannan, R.J. Butcher, J.P. Jasinski, Polyhedron 14 (1995) 3641.
[28] R. Oilunkaniemi, R.S. Laitinen, M. Ahlgren, J. Orgonomet. Chem. 623 (2001) 168.
[29] L.B. Kumbhare, V.K. Jain, R. Butcher, Polyhedron 25 (2006) 3159.
[30] S. Dey, V.K. Jain, A. Klein, W. Kaim, Inorg. Chem. Commun. 7 (2004) 601.
[31] S. Dey, V.K. Jain, B. Varghese, T. Schurr, M. Niemeyer, W. Kaim, R.J. Butcher, Inorg. Chim. Acta 359 (2006) 1449.
[32] V.K. Jain, S. Kannan, E.R.T. Tiekink, J. Chem. Soc., Dalton Trans. (1992) 2231.
[33] K. Umakoshi, Y. Yamauchi, K. Nakamiya, T. Kojima, M. Yamasaki, H. Kawano, M. Onishi, Inorg. Chem. 42 (2003) 3907.
[34] S. Dey, V.K. Jain, S. Chaudhury, A. Knoedler, F. Lissner, W. Kaim, J. Chem. Soc., Dalton Trans. (2001) 723.
[35] Powder diffraction File No. 43-1294, compiled by JPCDS, International Centre for Diffraction Data, USA, 1986.
[36] Powder diffraction File No. 29-0970, compiled by JPCDS, International Centre for Diffraction Data, USA, 1986.
[37] S. Dey, V.K. Jain, Platinum Met. Rev. 48 (2004) 16.
[38] D.D. Perrin, W.L.F. Armarego, D.R. Perrin, Purification of Laboratory Chemicals, 2nd ed., Pergamon, Oxford, 1980.
[39] V.I. Bakhmutov, J.F. Berry, F.A. Cotton, S. Ibragimov, C.A. Murillo, Dalton Trans. (2005) 1989.
[40] F.R. Hartley, The Chemistry of Platinum and Palladium, Wiley, New York, 1973.
[41] A.D. Ryabov, V.A. Polyakov, A.K. Yatsimirsky, J. Chem. Soc., Perkin Trans. II (1983) 1503.
[42] W.A. Herrmann, C. Brossmer, K. Öfele, C.P. Reisinger, T. Priermeier, M. Beller, H. Fischer, Angew. Chem., Int. Ed. Engl. 34 (1995) 1844.
[43] A.J. Costanza, R.J. Coleman, R.M. Pierson, C.S. Marvel, C. King, J. Poly. Sci. XVII (1955) 319.
[44] M. Bochmann, K.J. Webb, M.B. Hursthouse, M. Mazid, J. Chem. Soc., Dalton Trans. (1991) 2317.
[45] M. Akiba, M.V. Lakshmikantham, K.-Y. Jen, M.P. Cava, J. Org. Chem. 49 (1984) 4819.
[46] W.A. Herrmann, C.E. Zybill, in: W.A. Herrmann (Ed.), Synthetic Methods of Organometallic Chemistry and Inorganic Chemistry, vol. 4, Georg Thieme Verlog, Stuttgart, 1997, p. 205.
[47] G.M. Sheldrick, SHELXS-97, Program for Crystal Structure Determination, Universitäet Göttingen, Göttingen, Germany, 1997.
[48] G.M. Sheldrick, SHELXL-97, Program for Refinement of Crystal Structures, Universitäet Göttingen, Göttingen, Germany, 1997.